WATER-OIL RELATIVE PERMEABILITIES IN THE CASE OF A MIXED-WET CARBONATE RESERVOIR: INFLUENCE OF EXPERIMENTAL CONDITIONS

D.G. Longeron, L. Cuiec
Institut Français du Pétrole, Rueil-Malmaison, France
F.A. Yahya
Abu Dhabi National Oil Company, Abu Dhabi, U.A.E.

ABSTRACT

This paper describes a comparison of water-oil relative permeability curves obtained by the "Unsteady-State" technique with core samples from a mixed-wet carbonate oil reservoir located in the Middle East.
Coreflood tests were conducted firstly at standard (room) conditions, with synthetic fluids, using five cleaned core samples and, secondly, at reservoir conditions with a restored composite-core, built with the cores previously studied at room conditions. In addition, history matching of the coreflood tests was performed using a one-dimensional two-phase numerical model. Capillary forces were taken into account through an imbibition capillary pressure curve obtained separately by the "Porous Plate" technique adapted to reservoir conditions.
It has been demonstrated that the history matching of the coreflood test at a rate equivalent to the field rate is very sensitive to the spontaneous imbibition capillary pressure curve. The effect of the restoration of the reservoir conditions on the shape and the level of relative permeability curves has also been quantified. The residual oil saturation, S_{orw}, is 10% lower, and the relative permeability curves are more favorable at reservoir conditions than at room conditions.

Finally, this paper emphasizes the need to restore reservoir conditions and to numerically interpret coreflood tests when determining relative permeability curves for a mixed-wet carbonate reservoir.

1. INTRODUCTION

The Asab field is located in Abu Dhabi, United Arab Emirates, approximately 150 kilometers southwest of Abu Dhabi City. The Asab structure is 30 kilometers long and 10 kilometers wide. Production has been established from the Lower Cretaceous carbonates of the Thamama group, Zones A, B and C. The Thamama Zone B is the most important with regard to oil initially in place, cumulative oil production and oil production rate. This Zone B has been divided into six facies, with the M2 facies being the largest. Since the reservoir is subjected to waterflooding, the determination of water-oil relative permeability curves is essential for the predictive simulation of reservoir response.

This paper describes the results of a laboratory study performed in order to determine a set of k_{ro}-k_{rw} curves under conditions as representative as possible of the reservoir conditions for the M2 facies. In addition, a comparison of the curves obtained at standard conditions is given. The purpose is to evaluate the discrepancy between the two procedures, room versus reservoir conditions. The work described here is a part of a large laboratory study aiming to determine the wettability (1) and the electrical properties (m and n coefficients) of the rock samples from the Asab field (2). These previous papers have shown that the wettability of the reservoir rock is, on the whole, of a heterogeneous nature. For the M2 facies considered in this study, it has been demonstrated that the rock is mixed wet (i.e. spontaneous displacement of one fluid by the other is possible in both directions), with on the whole a clear preferential affinity for oil (1).

In such a case, the determination of water-oil relative permeability poses particular problems, as demonstrated by Labastie et al (3), Heaviside et al (4) and Mohanty and Miller (5). In this situation, found in many reservoirs, the well established scaling criteria for cores of well defined wettability no longer hold. A bibliographic review on the effect of wettability on waterflooding has been compiled by Anderson (6) and by Morrow (7). More recently, Jadhunandan and Morrow (8) demonstrated that a systematic increase in oil recovery by waterflooding occurred with change in wettability from water-wet to near neutral wettability.

The tests discussed in this paper are of the "Unsteady State" type. Waterflooding tests were conducted firstly at standard conditions with five cleaned core samples and, secondly, at reservoir conditions with a restored composite-core built with the cores previously studied at room conditions. The aspects concerning representative wettability and a valid method of reproducing the flow process, low flow rate (LFR) versus high flow rate (HFR), are discussed. To reduce the degree of freedom in the history matching of waterflood tests, capillary forces were taken into account through an imbibition capillary pressure curve measured separately at reservoir conditions by the "Porous Plate" technique.

2. GENERAL DESCRIPTION OF THE EXPERIMENTAL APPROACH

After the rock samples had been selected, the study included three main parts: wettability evaluation, coreflood tests (room and reservoir conditions) and capillary pressure measurements. Table 1 gives the core properties of the samples selected after CT scanning examination to check their homogeneity.

2.1. Wettability Evaluation

This evaluation was made upon reception, after cleaning and after restoration (i.e. after cleaning, saturation with reservoir fluids and aging).
The Amott method based on spontaneous and forced displacements was used. A full description is given in Reference 1.

2.2. Coreflood Tests at Room and at Reservoir Conditions

The unsteady displacement method was chosen because it is the most common method used in the petroleum industry. In addition, it is fast and resembles, at least qualitatively, the flooding process in the field. But it is an indirect method since the relative permeabilities are not measured but calculated from effluent and pressure drop data using the "Unsteady State" technique (JBN method) or its variants. This method is based on three assumptions:

- The core is homogeneous and linear,
- The flow is stable and one-dimensional,
- Capillary pressure effects are negligible compared to viscous effects.

Often these assumptions are not met, but in many laboratories, coreflood tests are interpreted using a one-dimensional coreflood simulator taking into account capillary forces. This point is discussed in Section 4.

- **Relative permeability measurements at room conditions**

After cleaning, the five plugs were saturated with synthetic formation brine, and the pore volume and brine permeability were measured. Then, the cores were flooded with a high-viscosity refined oil (μ_o = 68 cP) to establish Swi. The high-viscosity oil was miscibly displaced by a refined oil (Marcol 52, μ_o = 16.6 cP). Finally, the formation brine was injected at high constant flow rate (Q_w = 60 cm^3/hr) to minimize the possible capillary effects.

- **Relative permeability measurements at reservoir conditions**

After measurements at room conditions, the five plugs were cleaned again and individually coated with a low-melting-point alloy (Bi-Sn, melting temp. = 138°C). After the end-faces had been lathed, the cores were butted together under axial stress. Special care was taken to obtain an excellent capillary continuity without any bridging material. Arrangement of the composite-core with its characteristics is given in Table 2.

The composite-core was mounted in a triaxial core-holder cell, and the successive steps were performed:

a. after the composite-core had been evacuated, it was saturated with brine;
b. the brine was displaced by a high-viscosity refined oil to obtain S_{wi}, then the refined oil was miscibly displaced by stock-tank oil at room temperature;
c. the composite-core was heated to reservoir temperature (121°C) at 2600 psi of net overburden pressure, and stock tank oil was miscibly displaced by recombined reservoir oil at a pressure of 2900 psi (higher than the bubble point pressure);
d. the rock-fluids system was left for 14 days at 121°C and 2900 psi of pore pressure to restore the in-situ surface properties of the rock;
e. formation brine was injected at constant high flow rate (150 cm^3/hr); effluent production and pressure difference across the core were continuously measured and recorded.

After this HFR test, the core was cleaned again and steps a, b, c, and d were repeated. Then a second waterflood was performed at low flow rate (3 cm^3/hr). This flow rate was assumed to give a displacement velocity close to the one occurring in the field. After 3.4 pore volume of brine had been injected, higher flow rates were applied, up to 150 cm^3/hr, to evaluate the additional oil recovery and to measure the end-point of water relative permeability.

2.3. Capillary pressure measurements

This part was performed using the Porous Plate technique adapted to reservoir conditions. The equipment and procedures are described in Ref. 9. In spite of the long duration of the tests (one month for drainage and 2 months for imbibition) this technique was chosen because it gives a uniform saturation profile at each capillary equilibrium and a microscopic distribution of fluids as close as possible to the field one. In our procedure, the core was initially 100% saturated with formation brine, and the first drainage was performed by increasing the oil pressure, step by step, while the brine pressure remained constant. Eight capillary equilibria were performed in drainage, up to 29 psi of oil-brine capillary pressure. Then, the imbibition sequence was conducted by reducing the oil pressure (capillary pressure decreasing) to zero capillary pressure. Capillary equilibrium was considered to have been reached when the variation of saturation was lower than 0.1% PV per day for a given capillary pressure. The capillary pressure curves measured are displayed in Figure 1. There was only a water wet diaphragm in the equipment; consequently, it was not possible to obtain the forced part of the imbibition capillary pressure curve. This forced imbibition capillary pressure curve was deduced from numerical simulations (history matching) as described in Section 4.

3. THE RESULTS

3.1. Amott Wettability Indices

The following Table summarizes the average values that were obtained for the three situations (at reception, after cleaning and after restoration). Experiments were performed with three samples from the facies considered.

Wettability Indices	At Reception	After Cleaning	After Restoration
I_W (water wett. index) I_O (oil wett. index)	0.08 0.29	0.12 0.10	0.07 -0.33
$WI = I_W - I_O$	-0.21	+0.02	-0.26

From these figures, it may be seen that the wettabilities upon reception and after restoration were found to be satisfactorily similar (mixed wet with a preferential affinity for oil, for the M2 facies considered in the present study). A bland waterbase drilling mud was used, and the samples were very well wrapped and sealed to prevent any contact with the atmosphere, any oxidation, etc. It was also established that the wettability deduced from tests performed at 80°C, at atmospheric pressure and with stock tank oil was similar to the one deduced from tests performed under full reservoir conditions (1).

Consequently, the preserved and the restored samples were considered to be representative of the reservoir rock, as far as surface properties were concerned.

After cleaning, the wettability was found to be neutral but still of a mixed nature. Considering the solvents used (toluene, toluene-methanol mixture, chloroform, etc.) and the procedure used (forced displacement at 80°C), it can be concluded that a fraction of the surface of the rock contains hydrophobic material strongly linked to the solid (or hydrophobic surface sites ?).

3.2. Relative Permeabilities

The fluid properties together with experimental conditions are compared in Table 3. The five relative permeability curves obtained at room conditions are given in Figure 2. Despite the variation of S_{wi}, they are well grouped and can be reconciled in a single set of curves by using the standard reduced water saturation $S_w* = (S_w - S_{wi})/(1 - S_{wi} - S_{orw})$.

Figure 3 gives the oil recovery curves as a function of cumulative water injected for the waterflood tests at reservoir conditions. At high flow rate, the water breakthrough occurred later than at low flow rate (4% PV difference in oil saturation). This difference remained practically constant during the low flow rate test. But after the capillary number had been increased by increasing the flow rate, the S_{orw} value was practically the same (28.0% PV) for both tests. The relative permeability curves obtained directly from the HFR test (JBN technique) are plotted in Figure 4 and compared to the average set of curves obtained at room conditions. This clearly shows that oil relative permeability is more favorable at reservoir conditions (HFR) than at room conditions. In addition, the water relative permeability curve at reservoir conditions is quite far below the one obtained at room conditions, giving a more favorable displacement of oil by water. Obviously, these observations needed to be confirmed by history matching, especially for the LFR test at reservoir conditions. This part is developed in the next Section.

4. HISTORY MATCHING OF THE COREFLOOD TESTS AT RESERVOIR CONDITIONS

The purpose of this part was:

a) to check whether the capillary effects were actually negligible compared to viscous effects during the HFR test and,

b) to see if a single set of kr curves was able to correctly reproduce the experimental data for both HFR and LFR tests.

The approach can be summarized as follows :

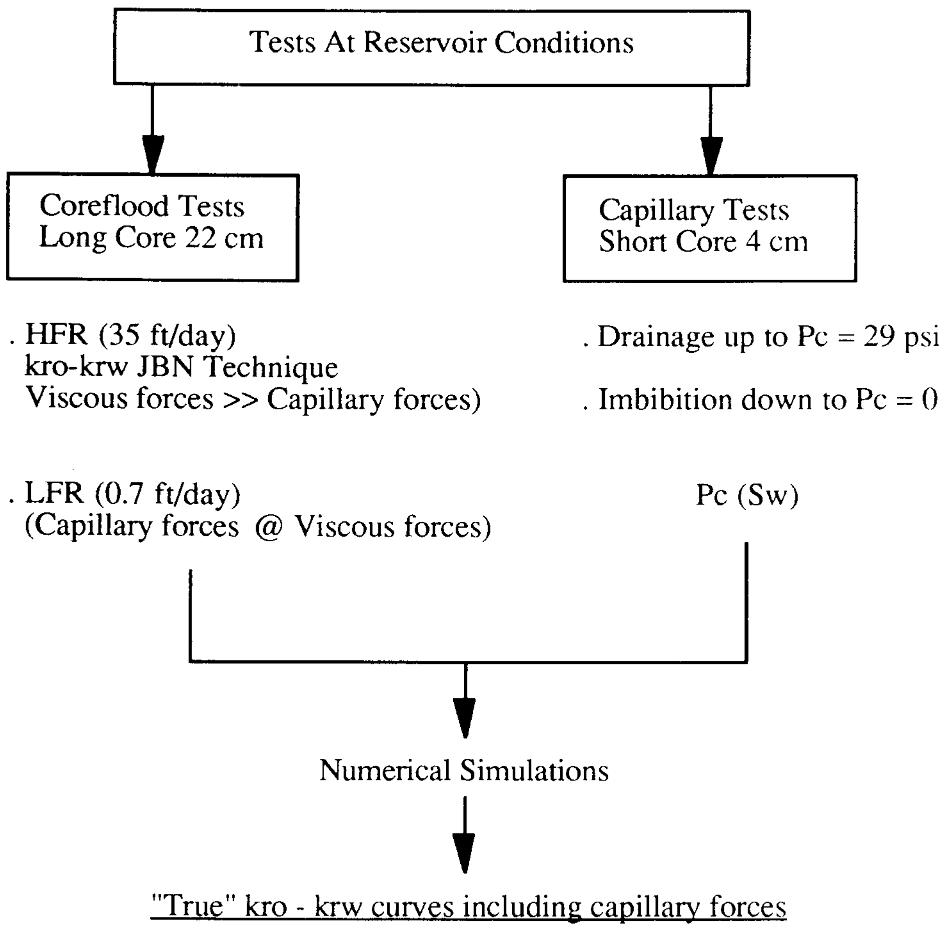

The rock sample was subdivided into 40 elementary blocks, corresponding to a space step, $\Delta x = 0.545$ cm. The numerical model gives, as a function of time (or cumulative volume of water injected), the oil recovery and the pressure difference across the core. These quantities are directly compared with laboratory measurements. It also gives the saturations calculated at the center of each elementary block. The description of the model and the initial and boundary conditions corresponding to the coreflood tests (forced imbibition at constant flow rate) are given in Reference 10.

For the HFR test, two numerical simulations were carried out:

Simulation No. 1 - HFR Test - Zero Capillary Pressure
This was done to verify the calculation of k_{ro}-k_{rw} values obtained by the JBN technique. An excellent agreement was obtained between predicted and measured oil recovery and ΔP, indicating the consistency of the experimental kr values.

Simulation No. 2 - HFR Test - Consideration of Capillary Pressure
The input data were identical to those used for Simulation No. 1, but the imbibition capillary pressure shown in Figure 5 was added. To obtain a good agreement between predicted and measured data (see Figures 6 and 7), it was necessary to modify significantly the oil relative permeability curve, as shown in Figure 8. The water relative permeability was unchanged.

Additional simulations were performed to evaluate the sensitivity of the model's response to the level of capillary pressure. Finally, by a "trial and error" process, the best fit was observed with the P_c curve shown in Figure 5, which differs slightly from the experimental one in the vicinity of Swi. No sensitivity was observed when using various negative (forced) capillary pressure curves in the Sw = 52 to 72% PV range (Figure 5).

Simulation No. 3 - LFR test
The input data were identical to those used for Simulation No. 2, except for the flow rate. An acceptable fit (± 1% in oil recovery) was obtained using the set of kr - P_c curves determined from Simulation No. 2. Various attempts were made to improve the fit between predicted and measured oil recoveries. Minor modifications of the P_c curve were made, especially in the negative part of the imbibition P_c curve (see Figure 5). The best fit shown in Figure 9 was obtained using the modified k_r curves shown in Figure 8 and the P_c curve shown in Figure 5 (LFR - Simulation No. 3). Finally, the comparison of the k_r curves, for room versus reservoir conditions is given in Figure 10.

5. ANALYSIS AND DISCUSSION OF THE RESULTS

• Connate Water Saturation and Residual Oil Saturation

The different laboratory procedures to establish the connate water saturation of the core samples lead to similar values of S_{wi}:

S_{wi} = 18.6 % by capillary drainage at reservoir conditions,
S_{wi} = 19.2 % by flooding with high viscosity oil (for the long core),
S_{wi} = 16.3 % (average) by flooding the five plugs.

Starting with similar values of S_{wi} , the ultimate residual oil saturation, S_{orw}, is 28% at reservoir conditions instead of 38% (average) for plugs at room conditions. This difference is related to the different experimental conditions (wettability, flow rate and viscosity ratio). Since this study did not aim to separate the effect of each parameter, it is impossible to conclude on the more important effect. However, to illustrate the effect of capillary forces, whose action is preponderant in waterflooding at low flow rate, Figures 11 and 12 compare the S_w profiles at different times of water injection.

Figure 11 (HFR)
Before the water breakthrough, the saturation front is very sharp. For instance, the saturation profile obtained at 0.2 PV of water injection shows that the water has penetrated up to 12 cm from the inlet face and S_w has increased from 19.2% (S_{wi}) to about 50% over a distance of 2 cm. After the water breakthrough, S_w decreases steadily as a function of distance from the inlet side (0.4 PV). At the end of displacement corresponding to a volume of 6 PV water injected, S_w is uniform (S_w = 72%) indicating complete sweeping of the sample.

Figure 12 (LFR)
Before the water breakthrough (0.1 PV), the front is spread over a distance of about 16 cm, corresponding to three-quarters of the length of the sample. Shortly after the water breakthrough (0.3 PV)) a decrease is observed in S_w as a function of the distance from the inlet side of the sample, except over the 4 cm close to the outlet side.
This is evidence of a capillary end-effect (retention of wetting fluid) associated with the capillary discontinuity at the downstream face of the sample (P_c = 0). This relatively slight capillary end-effect is completely nullified at the end of the test, corresponding to 3.4 PV of water injected. However, after 4.2 PV of water

injected, waterflooding is not complete, because the average water saturation is 65% PV, which is lower than the maximum value, $S_W = 72\%$, at which $k_{ro} = 0$. This maximum value is reached only after a large number of pore volumes of water injected.

- **Capillary pressure and relative permeabilities**

The capillary pressure measured in imbibition is low (less than 0.1 psi) in a wide range of water saturations. According to normally accepted criteria, the shape of the P_c (S_W) curve indicates that the formation exhibits mixed wettability or preferential wettability for oil. Yet the influence of capillary forces is not negligible on the results of displacement of oil by water. The relative permeabilities calculated by the JBN method must necessarily be corrected for this effect.

The shape of the relative permeability curves resulting from the numerical adjustment taking into account the capillary forces also indicates that the rock is not water wet. The following is an evaluation of the results of this study according to Craig's criteria (11).

Criteria	Water Wet	Oil Wet	Facies M2
connate water saturation, in % PV	>20-25%	generally < 15% frequently <10%	16 to 19%
saturation where k_{ro} and k_{rw} are equal	$S_W > 50\%$	$S_W < 50\%$	$S_W = 46\%$
k_{rw} at S_W maximum	generally < 0.3	> 0.5	0.43

CONCLUSIONS

. This work showed that unsteady relative permeabilities in a mixed wet core strongly depend on the experimental conditions.

. Conventional tests at room conditions and at high flow rate gave higher residual oil saturation values and less favorable relative permeabilities than those obtained at representative reservoir conditions.

. A single set of relative permeability curves was able to correctly predict both high flow rate and low flow rate tests conducted at reservoir conditions. But in such a case, simulations were very sensitive to the positive (spontaneous) part of the imbibition capillary pressure curve.

. Even at high flow rate, the influence of capillary forces was not negligible in the waterflood process for a mixed-wet porous medium. The standard scaling criterion appropriate for strongly water wet system is no longer valid for the mixed-wet core tests reported here. By ignoring the capillary pressure effects, the relative permeabilities are too pessimistic. This may induce a considerable impact on the reservoir engineering calculations.

. It is strongly recommended to determine experimentally the imbibition capillary pressure curve to improve the liability in the numerical simulations. Another way is to use continuous in-situ saturation monitoring to directly compare the predicted saturation profiles with measured ones.

ACKNOWLEDGMENTS

The authors are indebted to the Abu Dhabi National Oil Company (ADNOC) for having given permission to publish these results.

REFERENCES

1. Cuiec, L. and Yahya, F.A. : "Wettability of Asab Reservoir Rock : Comparison of Various Evaluation Methods-Role of Lithology". SCA Paper No. 9109 - Fifth Ann. Techn. Conf., San Antonio, TX, 1991.
2. Longeron, D. and Yahya, F.A. : "Laboratory Measurements of Cementation Factor and Saturation Exponent Under Reservoir Conditions on Asab Rock Samples". SCA Paper No. 9117 - Fifth Ann. Techn. Conf., San Antonio, TX, 1991.
3. Labastie, A., Guy, M., Delclaud, J.P. and Iffly, R. : "Effect of Flow Rate and Wettability on Water Oil Relative Permeabilities and Capillary Pressure", SPE Paper No. 9236 (1980).
4. Heaviside, J., Brown, C.E. and Gamble, I.J.A. : "Relative Permeability for Intermediate Wettability Reservoirs", SPE Paper 16968 (1987).
5. Mohanty, K.K. and Miller, A.E. : "Factors Influencing Unsteady Relative Permeability of a Mixed-Wet Reservoirs Rock", SPE Paper No. 18292 (1988).
6. Anderson, W.G. : "Wettability Literature Survey - Part 6 : The Effects of Wettability on Waterflooding", J.P.T. (Dec. 1987).
7. Morrow, N.R. : "Wettability and its Effect on Oil Recovery", J.P.T. (Sept. 1990).
8. Jadhunandan, P.P. and Morrow, N.R. : "Effect of Wettability on Waterflood Recovery for Crude Oil/Brine/Rock Systems", SPE Paper No. 22597 (1991).
9. Longeron, D., Argaud, M. and Féraud, J.P. : "Effect of Overburden Pressure, Nature and Microscopic Distribution of the Fluids on Electrical Properties of Rock Samples", SPFE (J), June 1989, pp. 194-202.

10. Chardaire-Rivière, C. et al. : "Simultaneous Estimation of Relative Permeabilities and Capillary Pressure", SPE FE (December 1992) pp. 283-289.
11. Craig, F.F. Jr. : "The Reservoir Engineering Aspects of Waterflooding", Monograph vol. 3, SPE of AIME, 1971.

Table 1 - Core Properties - M2 Facies

Sample No.	k_w (md)	Φ (%)	Purpose of Measurements
1	606	29.2	Wettability Evaluation
2	188	30.6	
3	331	24.9	Relative Permeability Measurements (Room and Reservoir conditions)
4	250	31.4	
5	230	30.9	
6	222	28.4	
7	183	29.8	
8	188	31.0	Cap. Press. Measurement (Reservoir Conditions)

Table 2 - Arrangement of the Composite Core (Coreflood Tests at Reservoir Conditions)

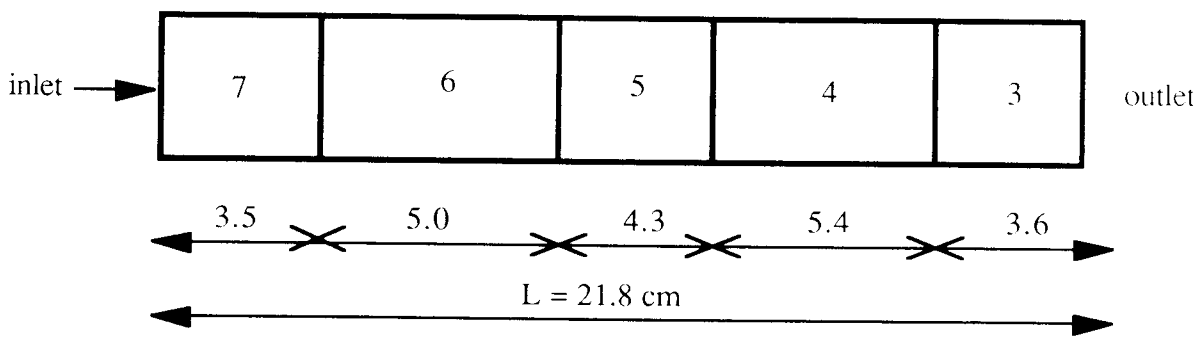

Measured values : k_w = 171 md ; Φ = 29.3 %

Table3 - Experimental conditions

	Room Conditions	Reservoir Conditions
Core Properties	k_w: 183 to 331 md Φ: 26.1 to 32.9%	171 md 29.3%
Thermodynamic conditions	T = 21°C p = atm. pressure	121°C 2900 psi
Net overburden pressure	500 psi	2600 psi
Brine viscosity Oil viscosity	1.44 cP 15.6 cP	0.43 cP 0.33 cP
IFT (interfacial tension)	22 mN/m	24.8 mN/m
Scaling Factor LμV (cm x cP x cm/min)	2	15 HFR 0.3 LFR
Capillary Number (μV/IFT)	0.9×10^{-6}	0.7×10^{-6} (HFR) 1.4×10^{-8} (LFR)
Swi	13.3 to 19.8% (average: 16.3%)	19.2 %
Sorw	35.3 to 40.5 % (average: 38.1%)	28.1%

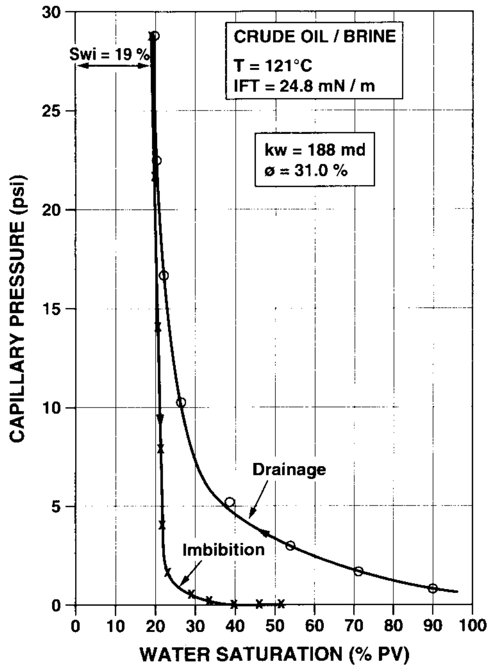

Fig. 1 Capillary pressures measured at reservoir conditions.

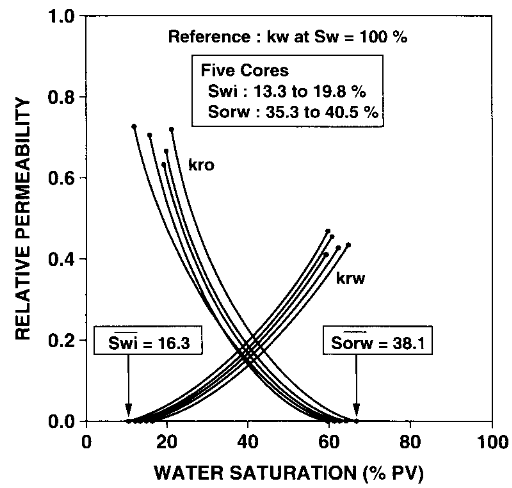

Fig. 2 Comparison of relative permeability (room conditions)

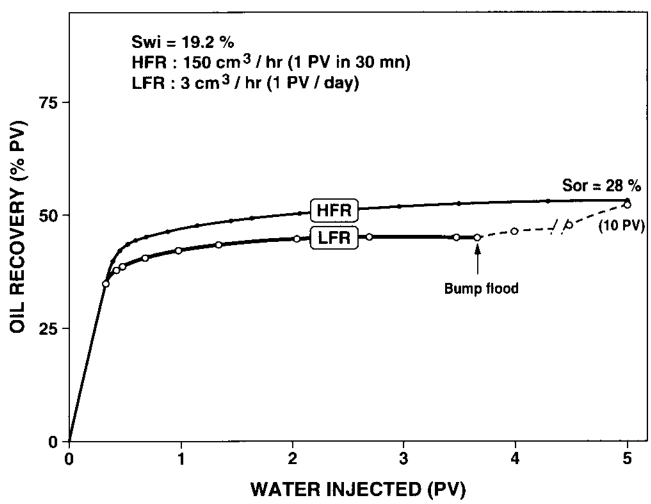

Fig. 3 Waterflood at reservoir conditions HFR versus LFR test.

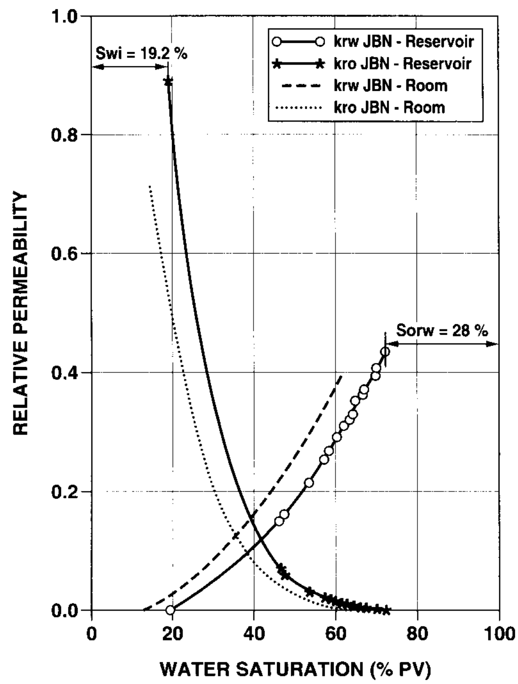

Fig. 4 Relative permeability curves. Room (average) versus reservoir conditions (HFR test)

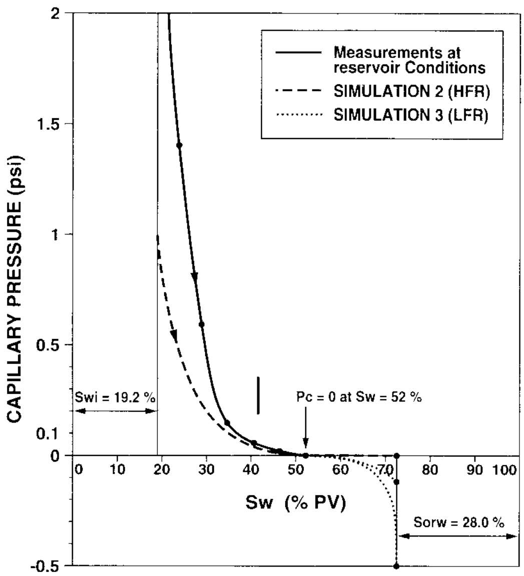

Fig. 5 Imbibition capillary pressure curves used for simulations.

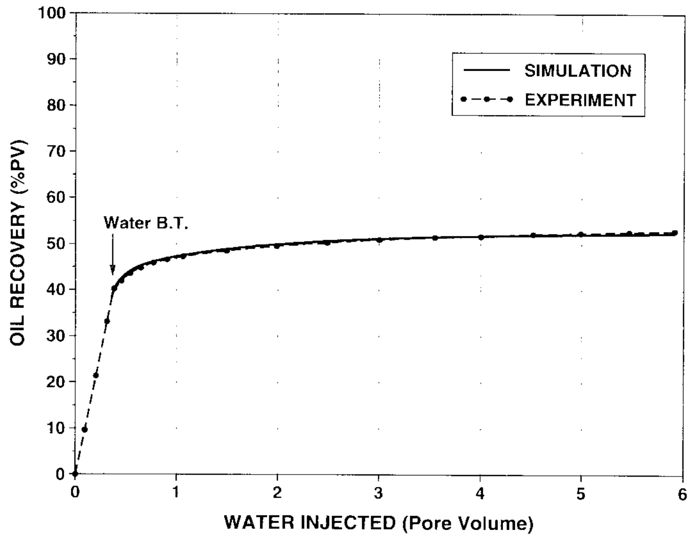

Fig. 6 HFR Test. Comparison of predicted and measured oil recoveries.

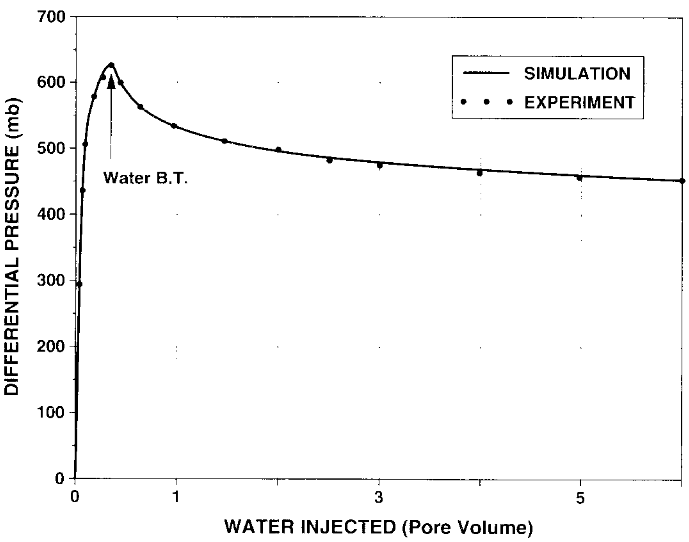

Fig. 7 HFR Test. Comparison of predicted and measured ΔP.

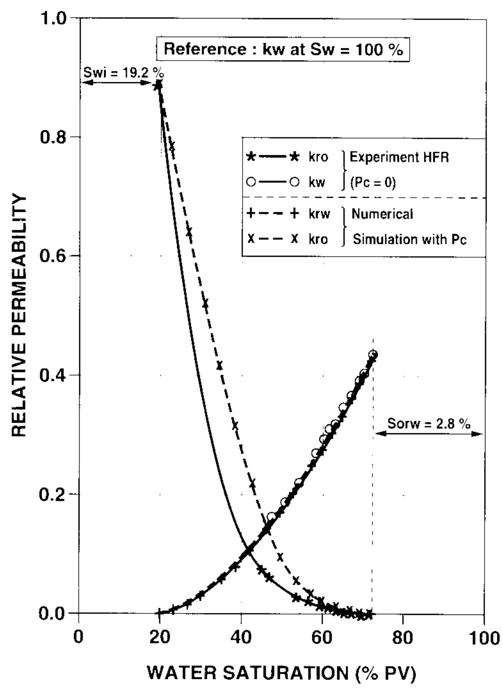

Fig. 8 Modification of kro due to consideration of Pc.

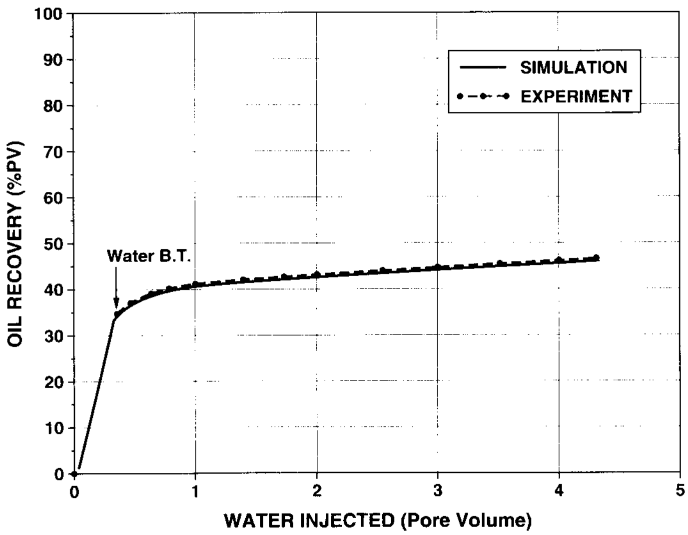

Fig. 9 LFR Test. Comparison of predicted and measured oil recoveries.

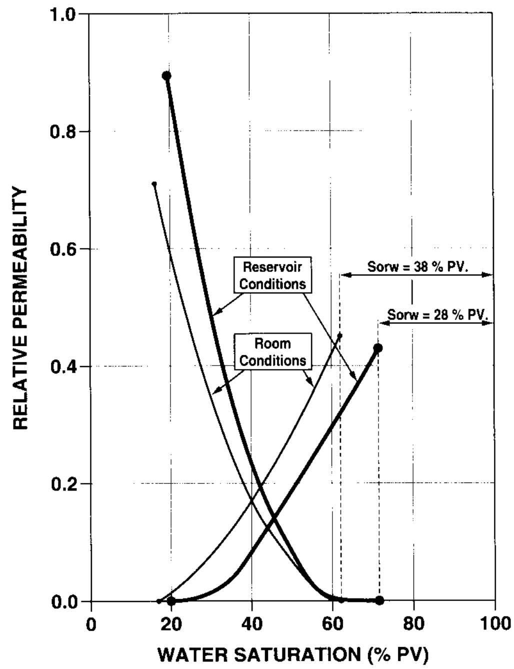

Fig. 10 Comparison of kr curves. Room versus reservoir conditions.

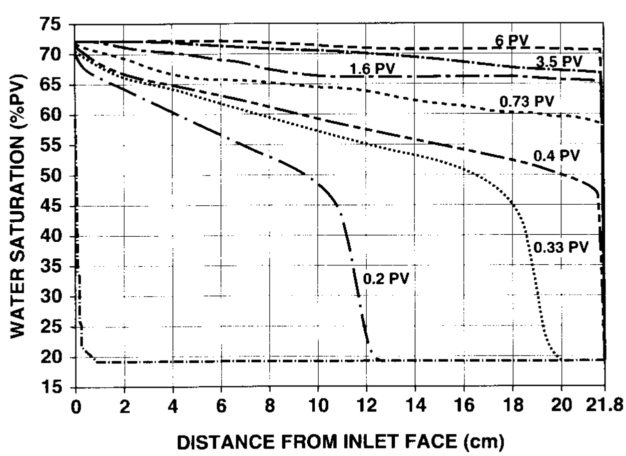

Fig. 11 HFR Test. Water saturation profiles at various injection times.

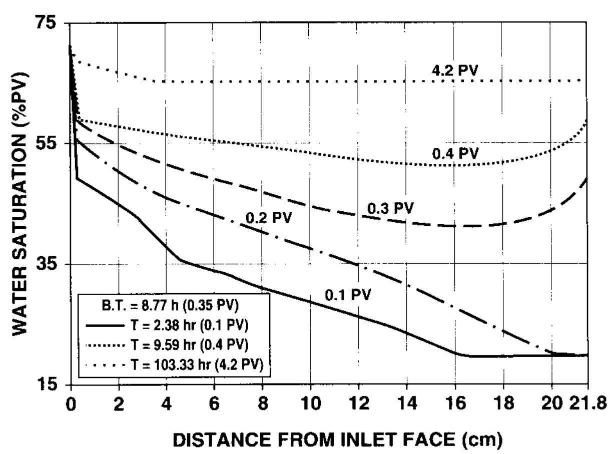

Fig. 12 LFR Test. Water saturation profiles at various injection times.